Rev. Adv. Mater. Sci. 48 (2017) 91-104

PARTICULATE REINFORCED ALUMINUM ALLOY MATRIX COMPOSITES – A REVIEW ON THE EFFECT OF MICROCONSTITUENTS

Kaka Ma[1], Enrique J. Lavernia[2] and Julie M. Schoenung[2]

[1]Department of Mechanical Engineering, Colorado State University, 1374 Campus Delivery, Fort Collins, CO 80523, USA
[2]Department of Chemical Engineering and Materials Sciences, University of California Irvine, 916 Engineering Tower, Irvine, CA 92697, USA

Received: January 17, 2017

Abstract. Particulate reinforced aluminum-based metal matrix composites (Al MMCs) continue to be of interest, partly due to their low density, but also because of their ability to provide tailored property combinations, such as high specific stiffness, specific strength and creep resistance. This article provides a review on the progress that has been made in the field of particulate reinforced Al MMCs during the past decade, paying particular attention to the influence of size and spatial distributions of the Al alloy matrix grains and the reinforcing particles on the mechanical performance of the composites. In addition, the current state-of-the-art as well as the challenges facing Al MMCs that involve heat treatable Al alloys as the matrix are addressed. Finally, our recent findings related to B_4C particulate reinforced 7xxx series Al alloy (Al-Zn-Mg) MMCs are also discussed.

1. INTRODUCTION

Modern engineering applications require the development of advanced materials that provide a broad spectrum of property combinations, such as: (i) high specific strength (light weight and high strength) and ductility for aerospace and automobile applications where fuel economy and enhanced engine performance become critical, (ii) low coefficients of thermal expansion (CTE) and high thermal stability for engine components that are exposed to high temperatures, (iii) superior wear resistance, high specific stiffness and satisfactory corrosion resistance in defense applications, and so forth [1–5]. Tailoring these property combinations is a great challenge if only monolithic material systems are considered. Hybrid materials such as metal matrix composites (MMCs) have been widely developed and investigated over the past fifty years, in an effort to achieve the aforementioned property combinations [1,2,4,6–10]. MMCs are generally referred to the materials consisting of a metallic matrix and ceramic reinforcement, such as oxides, borides and carbides [3]. The metallic matrix provides ductility, toughness, formability, thermal and electric conductivities while the ceramic reinforcement offers high hardness, strength, modulus, high-temperature durability, and low thermal expansion.

Aluminum (Al) based MMCs have attracted extensive interest because of their light weight and relatively low cost compared to copper-matrix and titanium-matrix composites [1,6,11–14]. In the 1990s, several review papers provided a summary of the processing approaches utilized to manufac-

Corresponding author: Kaka Ma, e-mail: Kaka.Ma@colostate.edu

ture Al MMCs, the strengthening mechanisms, deformation and fracture behavior in Al MMCs [2,3,15,16]. Partly due to the limited characterization techniques available during the last century, interpretation of processing-microstructure-performance correlation in Al MMCs was limited to a two dimensional (2D) point of view: each phase contributing its own properties to the macroscopic properties of the composite. Accordingly, the mutual influence between the Al alloy matrix and the reinforcement phase was not fully investigated. In recent years, increasing efforts have been devoted to the three-dimensional (3D) microstructural design in Al MMCs for performance improvement, in which the spatial distribution of both the matrix grains and the reinforcement particles, as well as the importance of phase connectivity in the properties of composites, have been better addressed than previous investigations [8,9,11,17–23].

It is generally accepted that the following mechanisms contribute to the strengthening of Al MMCs: (1) grain refinement of the metal matrix (Hall-Petch relationship: $\Delta\sigma_{H\text{-}P}=k_y/\sqrt{d}$), where d is the average grain size of the matrix and k_y is the Hall-Petch constant for the Al matrix alloy [7,9]; (2) load bearing effect from the hard reinforcement phase by an interfacial shear stress, which can be evaluated using the modified shear lag model: $\Delta\sigma_{L\text{-}T}=0.5\sigma_{ym}fs$, where σ_{ym} is the yield strength of the matrix, f is the volume fraction of the reinforcement and s is the aspect ratio of the reinforcing particles [7,9,24]; (3) Orowan dispersion strengthening from the presence of nanometric reinforcement particles or other possible dispersoids in the matrix [5,7,25]; and (4) Dislocations originating from geometrical constraints, i.e., geometrical necessary dislocations (GNDs), mismatch in coefficients of thermal expansion (CTE) between the matrix and the reinforcement phase (thermal contraction), and plastic deformation during processing [7,26]. A mathematical model, with a quadratic form, has been proposed to estimate the strengthening contribution of dislocations in composites [27]:

$$\Delta\sigma_{dis}=\sqrt{\left(\Delta\sigma_{OR}^{I}\right)^2+\left(\Delta\sigma_{OR}^{II}\right)^2+\left(\Delta\sigma_{GND}^{EM}\right)^2+\left(\Delta\sigma_{GND}^{CTE}\right)^2};$$

where $\Delta\sigma^{I}_{Or}$ is the contribution of the Orowan strengthening from the presence of nanoscale reinforcing particles; the second Orowan strengthening term $\Delta\sigma^{I}_{Or}$ takes into account the effect from precipitates or other dispersoids that are present in the Al matrix such as oxides or nitrides; $\Delta\sigma_{GND}^{EM}$ is the stress contribution due to strain gradient effect associated with GNDs caused by elastic modulus mismatch; $\Delta\sigma_{GND}^{CTE}$ accounts for the strengthening contribution due to GNDs caused by the thermal expansion mismatch between the matrix and reinforcement.

Fracture of Al MMCs also occurs through different mechanisms, including fracture of reinforcement particles, debonding between matrix and reinforcement phase, or void growth and crack propagation in the alloy matrix [15,17,18,28,29]. All the aforementioned findings suggest that the performance of the Al MMCs significantly depends on the microconstituents, i.e., selection of matrix alloys, reinforcement, size and spatial arrangement of the matrix grains and the reinforcing particles, and the interaction between individual microconstituents at the interface. One of the objectives of this article is to review the progress that has been made in the field of Al MMCs during the past decade, paying particular attention to the influence of spatial distribution of the different microconstituents, e.g., the Al alloy matrix grains and the reinforcing particles, on the mechanical performance of the Al MMCs. In addition, utilization of age hardened Al alloys, such as 2xxx series (Al-Cu), 6xxx series (Al-Si-Mg) and 7xxx series (Al-Zn-Mg), as the matrix phase in MMCs has brought in one more complexity to the system – precipitation behavior, which has raised additional scientific questions about these classes of composites [6,17,25,29–38]. With the presence of the reinforcing particles, could the precipitates in the composites form in the same sequence as those in the equivalent unreinforced matrix alloys? Will the kinetics of the precipitation be altered due to the defects caused by the addition of reinforcement, e.g., lattice strain in matrix, dislocations, segregation of solute atoms at interface, and so forth? Should the tempering conditions be modified to accommodate any difference in precipitation kinetics? In this context, the second objective of the present work is to address the current state and challenges facing Al MMCs that use heat treatable Al alloys as the matrix. Our recent findings for B_4C particulate reinforced 7xxx series Al alloy (Al-Zn-Mg) MMCs will also be discussed.

2. EFFECT OF MICROCONSTITUENTS

2.1. Selection of matrix alloys

Design of Al MMCs starts with choosing an appropriate class of Al alloys as the matrix according to the desired applications. Categorization of Al alloys has been well established based on the type of alloying elements, and they are grouped into non-heat-treatable or heat-treatable families. 5xxx series

Table 1. Characteristics of select Al alloys (data were obtained from [39]).

Matrix Alloy	Theoretical Density [g/cm^3]	Elastic Modulus [GPa]	Yield Strength [MPa]	CTE [10^{-6}/°C]	Cost [USD/kg]
Al 5083 (Mg-alloyed)	2.64-2.67	70-73.6	269-297	23.6-24.8	2.95-3.25
Al 6061 (Mg-Si alloyed)	2.67-2.73	68-74	193-290	22.7-23.9	2.93-3.23
Al 2024 (Cu alloyed)	2.75-2.78	72-75.7	345-381	23.2-24.4	3.2-3.52
Al 7075 (Zn-Mg alloyed)	2.77-2.83	69-76	359-530	22.9-24.1	3.03-3.33

(Al-Mg) alloys, one example of non-heat-treatable Al alloys, are moderate in strength (200-350 MPa) but possess excellent resistance to corrosion in aggressive atmosphere and seawater. Thereby, they are suitable as the matrix phase in composites for naval applications [39]. Some physical and mechanical data of select Al alloys are provided in Table 1 based on the Cambridge Engineering Selector (CES) database [39]. 2xxx series (Al-Cu), 6xxx series (Al-Si-Mg) and 7xxx series (Al-Zn-Mg) alloys belong to the heat treatable category and exhibit high strength achieved by heat treatment processes that consist of a solution treatment and an aging step, which are also commonly referred to as tempering. Starting with a supersaturated solid solution of the alloying elements in the Al matrix, precipitates form in sequence upon aging for these three classes of Al alloys. Those precipitates strengthen the materials by inhibiting dislocation motion through shearing mechanism or Orowan dislocation looping mechanism. 6xxx series alloys are superior to 2xxx and 7xxx series alloys in terms of corrosion resistance, although they do not have strength as high as 2xxx and 7xxx series alloys. 6xxx series alloys have typical applications in heavy duty structures, pipe, rail and marine uses. 7xxx series alloys possess the highest strength at ambient temperature among all series and thus are widely used in aircraft structures. 2xxx series alloys exhibit slightly lower strength than 7xxx series alloys but higher stress corrosion resistance. Therefore, they are promising candidates for matrix materials in MMCs for applications for aircraft as well. It is worthy to note that due to the dependence of precipitation behavior on heat treatments, care should be used when 2xxx, 6xxx and 7xxx series alloys are considered as matrix materials for applications at elevated temperatures or thermal cycling.

In addition to the intrinsic properties of the various Al alloys, spatial distribution of matrix grains with different sizes is essential to the design and performance of the composites. As grain boundaries could act as effective obstacles to dislocation motion, refining the grain size of the Al matrix improves the strength of the composites with a sacrifice in ductility [5,7,22,40]. Consideration of this grain size-dependent spatial arrangement of matrix phase has led to a novel concept named trimodal composites, consisting of nanocrystalline or ultrafine grained (UFG) Al matrix regions, coarse grained (CG) Al matrix regions, and reinforcing ceramic particles [8,20,21,23]. Blending in the CG Al matrix portion was originally formulated to improve the ductility of the matrix while the UFG region provides efficient obstacles for dislocation movement, such as grain boundaries and other crystalline defects. Fig. 1 shows a schematic diagram of the trimodal microstructure of the Al MMCs with micron sized reinforcing particles distributed within the UFG Al matrix [8,41]. The concept of a trimodal structure is both scientifically novel as well as technologically promising because it provides multiple controllable degrees of freedom that allow for extensive microstructure design such as the spatial distribution of the matrix grains and the reinforcing particles [8,22].

Our group has used cryomilling [42,43], one severe plastic deformation powder metallurgy approach, followed by different thermo-mechanical processing (TMP) routes, to fabricate Al MMCs with different spatial distributions of the Al matrix grains.

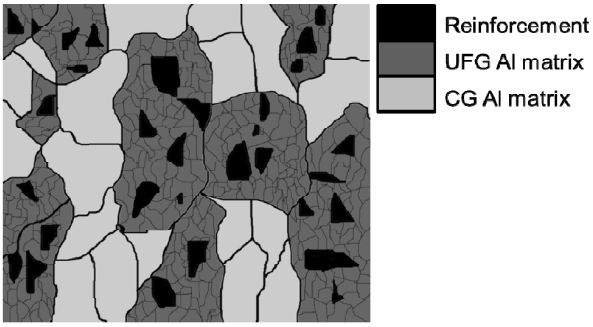

Fig. 1. Schematic diagram of a tri-modal Al MMC reinforced with micron-sized ceramic particles [8,41]. The light grey regions correspond to coarse grained (CG) Al matrix; The dark grey regions correspond to the ultrafine grained (UFG) Al matrix in which the solid grey lines denote grain boundaries; The black regions correspond to the ceramic reinforcement. Reprinted with permission from L. Jiang, K. Ma, H. Yang, M. Li, E.J. Lavernia and J.M. Schoenung // *JOM* **66** (2014) 898, (c) 2014 Springer.

A trimodal composite consisting of 10 wt.% B_4C with the particle size ranging from submicron to 2 μm, 40 wt.% UFG 5083 Al, and 50 wt.% CG 5083 Al exhibited an extremely high yield strength (up to 1065 MPa) under compressive load [20]. Fig. 2 shows the tensile properties at ambient temperatures that have been achieved in UFG or trimodal Al 5083 composites reinforced by B_4C particles [7,9,40]. The data are categorized into three different groups for the purpose of comparison. Group A are composites using B_4C particles with a size range of 1-7 μm as the reinforcing phase, and the weight percentage of each microstructural constituent is $f_{UFG}/f_{CG}/f_{reinforcement}$ = 40/50/10; the difference between each member in Group A is the TMP route. The composite processed by high strain rate forging (HSRF) exhibited slightly higher strength than the ones processed through quasi-static forging (QIF) due to the inhibition of dynamic recrystallization of

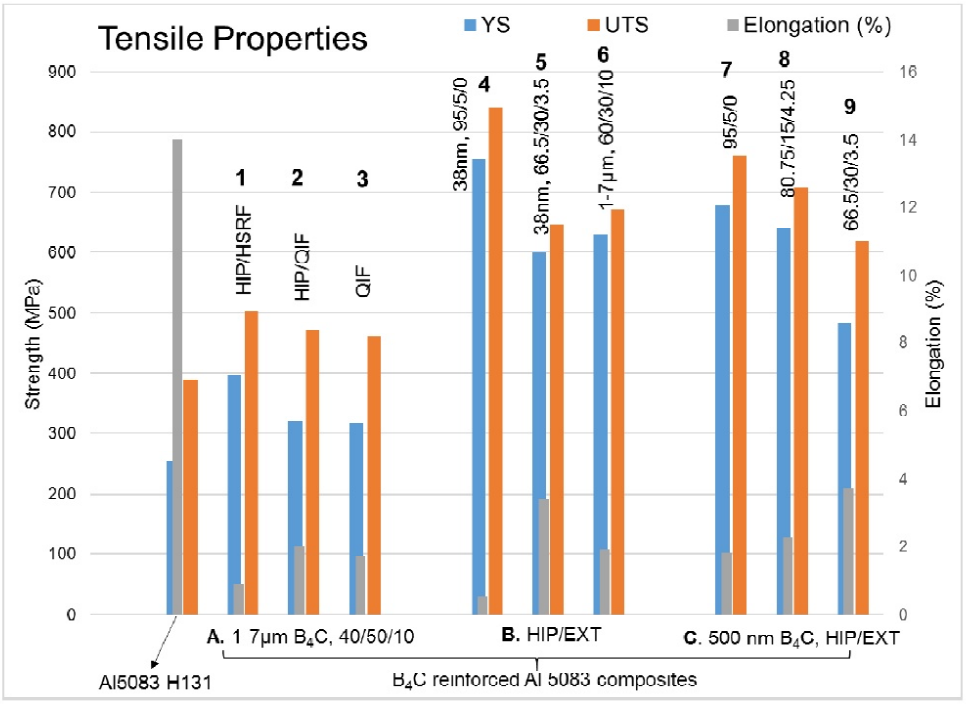

Fig. 2. Summary of tensile properties at ambient temperature achieved in B_4C reinforced Al 5083 composites compared to conventional Al5083 H131 [7,9,40]. The blue, orange and grey bars correspond to yield strength (YS), ultimate tensile strength (UTS) and elongation, respectively. Group A are composites using B_4C particles with a size range of 1-7 μm as the reinforcing phase, and the weight percentage of each microstructural component is $f_{UFG}/f_{CG}/f_{reinforcement}$=40/50/10; the TMP routes for each member in Group A are different from each other. HIP, HSRF, QIF, and EXT stand for hot isostatic pressing, high strain rate forging, quasi-isostatic forging, and extrusion, respectively. Group B are composites fabricated by HIP followed by extrusion. The size of the B_4C particles and the weight percentage of individual microstructural components for each member in Group B are different from each other. Group C are composites with submicron B_4C particles (mean size ~ 500 nm) processed by HIP/EXT. The difference between the members in Group C is the weight percentage of CG powder that was blended in before HIP.

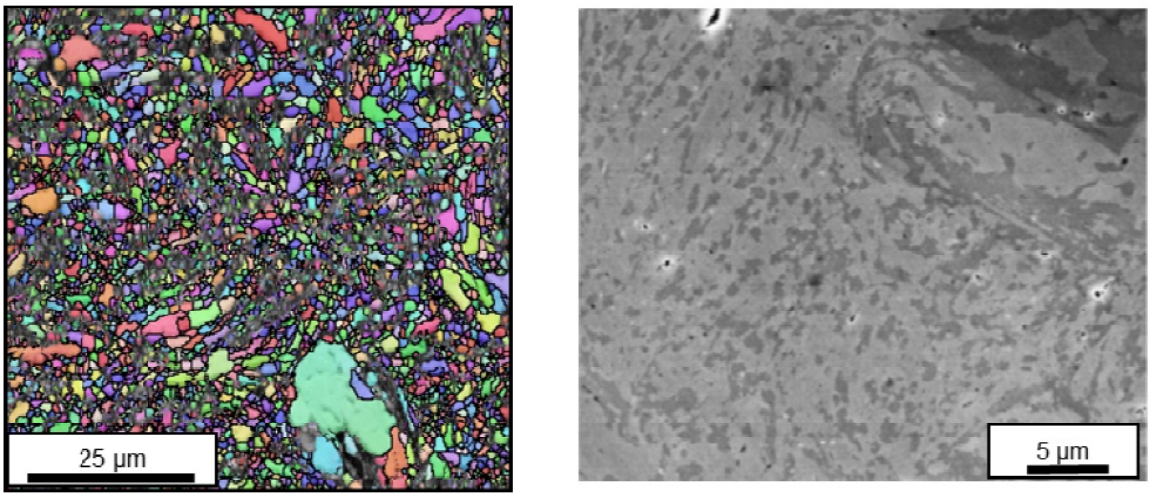

Fig. 3. Microstructure showing the gradient size distribution of the Al matrix grains. Reprinted with permission from H. Yang, E.J. Lavernia and J.M. Schoenung // *Philos. Mag. Lett.* **95** (2015) 177. (c) 2015 Taylor & Francis.

the Al matrix grains [40]. The results for the composites in Group B and Group C suggest that, for a given size and a given volume fraction of reinforcing particles, the fractions of the CG and UFG altered the tensile properties of the composites: the ductility of the composites increased as the fraction of CG increased, with a sacrifice in strength. The results in Fig. 2 also highlight the size effect of the B_4C particles, which is discussed in the next session.

In addition, the spatial arrangement of the Al matrix grain size is expected to influence the mechanical behavior of the composite. Our group proposed a novel powder metallurgy approach to create gradient microstructures in the Al matrix, which extended the concept of a bimodal grain size distribution to a broad and continuous distribution of grain sizes (100 nm to 3 μm) in the Al matrix powder, as shown in Fig. 3 [44]. A unique "interfingered" structure was created where the two starting phases were intermixed in a complex three-dimensional mesh. Geometric optimization simulation revealed that the synthetic microstructure could be achieved by the following sequence: (a) random sequential adsorption of coarse grains, (b) simulated annealing optimization algorithm to achieve desired clustering of coarse grains, and (c) fill the remaining space with UFG phase, as illustrated in Fig. 4 [45]. Hardness studies of this gradient microstructure at different length scales (macro-, micro- and nano-indentation) highlighted that the gradient microstructure is disordered locally, but homogenous macroscopically. The design of gradient microstructure in the Al matrix is expected to enhance the ductility of the composites [46].

2.2. Selection of reinforcement phase

A variety of oxides, carbides and borides have been utilized as the reinforcement phase in Al MMCs. The morphology of reinforcement in Al MMCs can be in a variety of forms: continuous or discontinuous fibers, whiskers, or particulates. The fabrication of continuous fiber reinforced MMCs often encountered the challenges of fiber damage, fiber-to-fiber contact, and microstructural nonuniformity during fabrication. The scope of this review article focuses on the particulate-reinforced composites, and the following discussion addresses the size effect and the spatial distribution of the reinforcing particles. Some selected physical and mechanical properties of commonly used ceramic reinforcements are summarized in Table 2 [39]. The structural efficiency of Al MMCs and the corresponding mechanical behavior are a function of the physical, thermal, and mechanical properties of the reinforcing phases. Selection of the ceramic reinforcement should follow a broad spectrum of criteria, including (a) density, (b) elastic modulus, (c) hardness, (d) thermal stability (i.e. any phase transformations at elevated temperatures), (e) coefficient of thermal expansion (CTE), (f) compatibility with matrix material (wettability, reaction with matrix, etc.), (g) size, (h) morphology, and (i) availability and cost. The chemical stability and compatibility of the reinforcements with the matrix material are critical for both

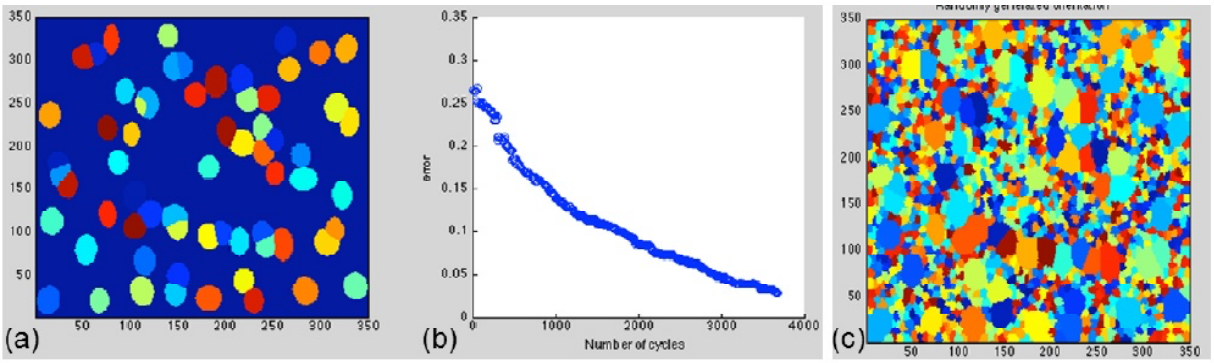

Fig. 4. Geometric optimization simulation revealing the formation of synthetic microstructure of gradient grain size distribution in Al matrix phase, courtesy of Dr. Kristopher Wehage [45].

Table 2. Characteristics of select reinforcement ceramics (data were obtained from [39]).

Reinforcement	Density [g/cm^3]	Elastic Modulus [GPa]	Hardness-Vickers [GPa]	CTE [10^{-6}/°C]	Cost [USD/kg]
Al_2O_3 (p)	3.94-3.96	450-460	8.83-9.81	7.7 -8.5	33.2-41.5
B_4C	2.35-2.55	440-472	31.4-39.2	3.2-3.4	60.1-89.2
TiB_2 (p)	4.43-4.52	500-545	25-32.4	4.6-4.7	20.7-41.5
SiC (p)	3.15-3.2	450-480	31.4-32.4	3.9-4.3	31.1-51.8
TiO_2	3.97-4.05	276-288	9.15-10.1	8.4-11.8	24.9-37.3
YSZ	5.2-5.9	97.5-103	2.54-2.81	6-8.8	18.7-27

Note: (p) denotes the particulate form.

the end application and during material fabrication. The CTE mismatch between the reinforcement and the matrix is an essential factor for composites that will be exposed to thermal cycling. Availability and cost should be also considered for commercialization. For instance, B_4C is superior to the other alternatives in terms of its low density (even lighter than the Al), high hardness and high stiffness. Al_2O_3 is thermally stable with the Al matrix and also is an economic choice due to its abundant resource in nature and lower cost relative to B_4C. TiB_2 also has emerged as an advantageous option because of its high modulus, resistance to mechanical erosion, and its effectiveness as a grain refiner [13,47].

2.2.1. Size effect

The significance of the size of the reinforcing particles has been investigated in various studies, particularly in powder metallurgy processed MMCs [7–9,14,48]. Coarse (micrometric) reinforcing particles effectively induce grain refinement in the Al matrix [49,50] and subsequently lead to strengthening of the matrix. Nevertheless, the micrometric ceramic particles are prone to act as stress concentrators that promote early nucleation of cracks and voids [41]. On the other hand, submicron or nano-scale reinforcing particles produce more homogeneous deformation with the presence of dislocation cells, if they are uniformly dispersed in the matrix; those ultrafine reinforcing particles are less prone to crack or damage during the synthesis or deformation processes [9,17,47,51]. However, nanometric reinforcements naturally tend to cluster due to the strong van der Waals forces between the particles because of their high surface to volume ratio; therefore, it becomes a challenge to homogeneously disperse the ultrafine reinforcing particles in the metal matrix. Our previous investigations have shown that mechanical milling is an effective approach in promoting uniform distribution of nanoscale and or submicron reinforcing particles [7,13,20,21]. Investigation into Al 5083 nanocomposites, with Al matrix grain size of 115 nm and B_4C reinforcing particle

size of 38 nm, suggested that the nanoparticles-reinforced composite possessed enhanced plasticity relative to the same material reinforced with micrometric particles, as shown in Fig. 2 [7]. Earlier studies on micrometric and nanoscale particulate reinforced composites indicated that CG matrix phase regions were needed in an effort to achieve any tensile plastic strain [40,41,52,53]. A more recent study on Al 5083 composites with submicron B_4C reinforcement demonstrated both enhanced strength and ductility compared to the previously published data by Zhang et al. and Vogt et al. on nanometric and micrometric trimodal composites [7,9,40], as illustrated in Fig. 2. Specifically, those three samples in Group A in Fig. 2 were reinforced with micrometric B_4C particles and have a larger volume fraction of CG phase (~ 50%) than the composites in Group C with submicron B_4C. The former showed tensile ductility <2% and ultimate tensile strengths <500 MPa, while the latter achieved elongation values of 2.3% and 3.7% in spite of the lower weight fraction of the CG phase. As compared to the nanometric B_4C reinforced composites that have the same nominal volume fraction of B_4C and CG phases, the composites with submicron B_4C particles also exhibited comparable tensile strengths and enhanced ductility, as demonstrated by the comparison between Sample 4 and Sample 7, and the comparison between Sample 5 and Sample 9 in Fig. 2. The size effect of the reinforcing particles is also essential in determining the deformation behavior in Al MMCs [15,29,54]. A previous study from our group proposed a novel diagnostic approach applying nanoscratch testing to elucidate the role of B_4C particle size in the plasticity mechanisms responsible for the behavior of composites [54]. The deformation mechanisms were classified into three categories as illustrated by the micrographs of the nanoscratch induced grooves and the corresponding schematic diagrams (Fig. 5): (i) for particles larger than 1 or 2 μm: transgranular cracking and crack branching dominates, because the large interfacial bonding area makes it difficult to displace the B_4C particles during the nanoscratch test; (ii) for particles with size of 500 nm to 1 μm: displacement and microcracking at the interface is predominant; and (iii) for ultrafine particles 50–500 nm in size: no apparent deformation occurred to the B_4C particles themselves or at the interfaces between the fine particles and the Al alloy matrix [54]. These nanometric B_4C particles have been either rolled over and subsequently pushed aside with the plastically deformed Al matrix or pushed downwards into the matrix.

Likewise, results from other studies on micrometric SiC particulate (SiC_p) reinforced 7075 composites using three different nominal sizes of SiC particles [36], also suggest opposite trends observed in tensile strength of the composites: minor increases in tensile strength were achieved for 5 μm-SiC and 13 μm-SiC while the tensile strength was decreased for 60 μm-SiC. In a later study on a nanometric-SiC_p reinforced Al 7075 composite [25], a significant drop in the hardness and tensile properties of the composites were observed due to agglomeration of nano-SiC particles and segregation of Mg in the vicinity of the nano-SiC_p and at Al grain boundaries. Hunt et al. [48] suggested that there was a relationship between the toughness of SiC_p reinforced 7000 series Al composites and the SiC_p-Al powder size ratio: for a given volume fraction of SiC_p, the toughness of the composite increased with an increasing SiC_p-Al powder size ratio as the interparticle distance decreased.

All of the above observations suggest that the size of the reinforcing particles influences the mechanical performance of the composites. However, the effect does not follow a simple linear trend, i.e., finer particle size of the reinforcement (e.g., nanometric) does not necessarily lead to improved mechanical properties since the spatial distribution also plays a critical role, as addressed in next session.

2.2.2. Spatial distribution

The majority of the research activities in discontinuously reinforced Al MMCs have aimed to produce a homogeneous and discrete distribution of the reinforcing particles due to the belief that favorable attributes, such as improved specific strength, stiffness and superior wear resistance, could be achieved through uniform distribution of the reinforcing particles [12,22]. Nevertheless, it has been widely noted that the reinforcing particles are prone to clustering, particularly for particles with fine size, which cause the mechanical properties of the MMCs to deteriorate. In addition to the size effect, recent studies have begun to pay more attention to the significance of spatial distribution of the reinforcement particles in the performance of the composites [8,18,56,57]. Unique design opportunities have been explored by controlling the arrangement of reinforcing particles at a mesoscopic scale within a given section of the material, specifically in terms of gradient and layered structures. The controlled inhomogeneous microstructures include reinforcement clustering microstructure, bi-continuous microstruc-

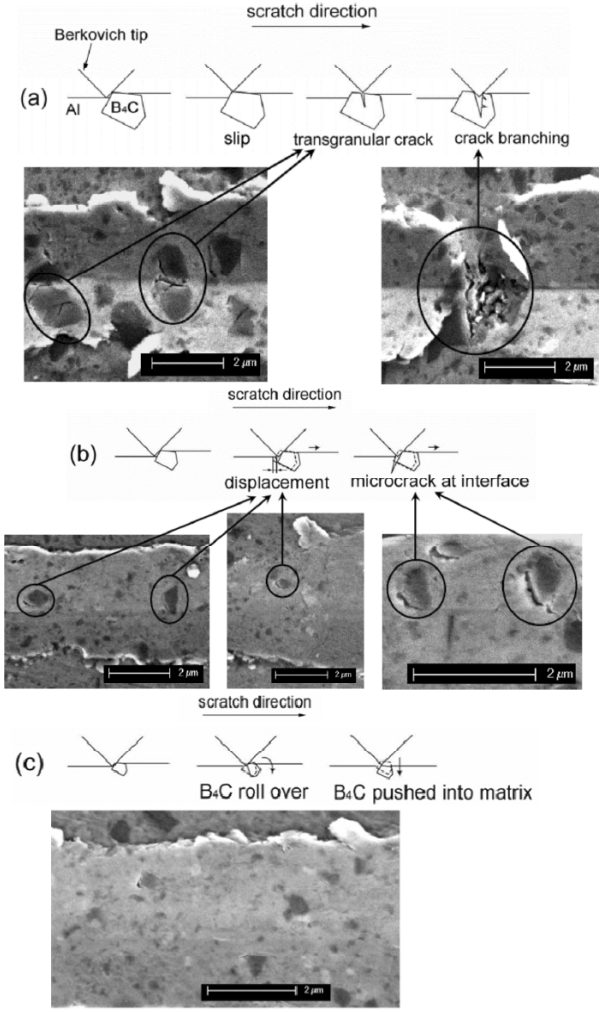

Fig. 5. Micrographs and the corresponding schematic diagrams showing the dependence of nanoscratch-induced deformation patterns on B_4C particle size, for particles: (a) larger than 1 or 2 μm; (b) 500 nm to 1 μm; and (c) 50–500 nm in size, respectively. Reprinted with permission from L. Huang, T.D. Topping, H. Yang, E.J. Lavernia and J.M. Schoenung // *Philos.Mag.* **94** (2014) 1754. (c) 2014 Taylor & Francis.

ture, interpenetrating microstructure, laminated microstructure, network microstructure, etc., in which the reinforcing phase is inhomogeneously distributed at the micro-scale but homogeneously or still not homogeneously distributed at the macro-scale [57]. These inhomogeneous microstructures exhibited significant improvements in fracture toughness, ductility and strength. One of our previous studies demonstrated a strategy of introducing spatial arrays of nano B_4C particles in Al MMCs [18]. A 26% increase in tensile strength, compared to an equivalent unreinforced material, was achieved by creating arrays of fiber-like zones that are rich in spherical nanoparticles of B_4C embedded in an ultrafine grained (UFG) Al alloy matrix, as demonstrated in Fig. 6. The fiber-like zone distribution of B_4C particles also led to a 30% increase in toughness when compared to a nanocomposite containing a homogeneous distribution of B_4C. Another study from our group on submicron B_4C particles reinforced UFG Al 5083 composite also exhibited that random-like dispersed B_4C network contributed to enhanced ductility [9].

Furthermore, a concept of functionally graded (FG) particle reinforced metal matrix composites was proposed based on spatial distribution of the reinforcement particles, in which the volume fraction of the reinforcement particles varies, either stepwise or continuously, across the section [11]. The gradient spatial distribution of the reinforcement particles allows for a controlled non-uniform microstructure with continuously changing properties, thereby expanding the usefulness of Al MMCs in applications where a combination of high surface wear resistance and high toughness of the interior bulk material is required. In addition, the gradient spatial distribution of the reinforcement particles minimizes thermal stresses, interface stresses, thermal mismatch between the reinforcement phase and the matrix, and consequently enhances thermal stability, and particle/matrix interface bonding in Al MMCs. Prabhu [56] investigated FG AA 7075 Al/SiC composites fabricated by the centrifugal casting technique, in which the micron-sized SiC particles were gradiently distributed from the surface to the core of the part. The hardness and wear resistance of the FG composites increased from the core to the surface as the particle volume fraction increased. Castro et al. [58] have studied the tensile and fracture toughness properties of centrifugally cast FG A356/SiC composites. The tensile strength increased in the region where the volume fraction of SiC was 20–30%, and it decreased in the region where the volume fraction of SiC was 30–40%. The fracture toughness decreased in the direction of increasing SiC volume fraction. The particle fracture was dominant over the particle/matrix debonding as the volume fraction of SiC increased in the composites. Lin et al. [59] have investigated the fracture toughness of the FG Al 2124/SiC composites processed by a metal forming process. They observed that the crack growth resistance increased from the higher SiC content layer to the lower one.

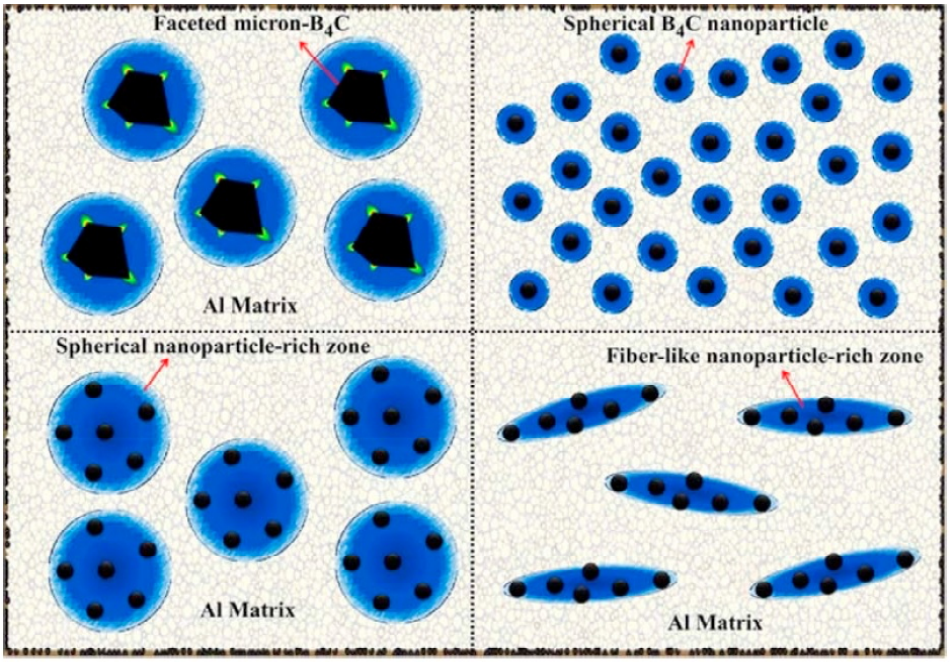

Fig. 6. Schematic diagram of the options for spatial distribution of B_4C particles in Al matrix. Reprinted with permission from L. Jiang, H. Yang, J.K. Yee, X. Mo, T. Topping, E.J. Lavernia and J.M. Schoenung // *Acta Mater.* **103** (2016) 128. (c) 2016 Elsevier.

3. AGE-HARDENABLE Al ALLOY COMPOSITES

This section provides a discussion on MMCs using age-hardenable Al alloys as the matrix phase. Previous investigations, as shown in Fig. 7, have so far reported mixed results on the mechanical properties of this class of Al composites. Both increases and decreases in the strength of the Al 7xxx series alloy matrix composites reinforced with either micrometric or nanometric scale ceramic particulates were observed compared to unreinforced Al 7xxx series alloys [6,29,31,36,37,60,61]. J. K. Shang et al. [60] and A. Ahmed et al. [6] observed a reduction in tensile strength of the composites compared to the alloy matrix. SiC particles (SiC_p) were used as the reinforcing phase in both studies, but with different mean sizes. Severe agglomeration occurred for the nanometric SiC_p. In addition, segregation of Mg was observed in the vicinity of the nano SiC_p particles and at Al grain boundaries. In contrast, a more recent study reported that a micrometric SiC_p (mean particle size ~ 20 μm) reinforced Al 7075 alloy composite fabricated by stir casting exhibited higher tensile strength and hardness relative to the matrix alloy [32].

McDanels reported that the matrix alloy and its temper condition were the predominant factors that control the yield strength, tensile strength and ductility in SiC reinforced heat treatable Al alloy composites [62]. The reinforcement affected the strength of composites, but only for those in which the whisker reinforcement was highly oriented. However, work by Carpenter et al. has shown severe segregation of Mg and formation of MgO precipitates at Al/SiC interfaces in a SiC-AA2024 MMCs [63]. The Mg segregation phenomenon has been well documented for monolithic Al-Mg alloys, and is generally attributed to vacancy-solute pair diffusion to boundaries due to the presence of a supersaturation of quenched vacancies. Therefore, it is worth noting that the addition of reinforcement phase does influence the mechanical properties of the composites by changing the chemistry in the Al alloy matrix due to segregation of prior solid solutes to Al/reinforcement interfaces, which eventually altered the precipitation kinetics in the heat treatable Al matrix alloy.

In spite of the aforementioned work on age-hardenable Al alloy-based composites [6,17,25,29–38], little research has been performed to systematically study the effect of the particulate reinforcement on the precipitation behavior. An early investigation revealed that the effects of matrix aging condition (i.e., matrix temper) on fracture toughness of 2xxx and 7xxx matrix alloys reinforced with SiC particulates were different from each other [33]. In the 7xxx series composites the fracture mode transited from particle cracking in under-aged condition to matrix and near matrix/SiC interface failure in

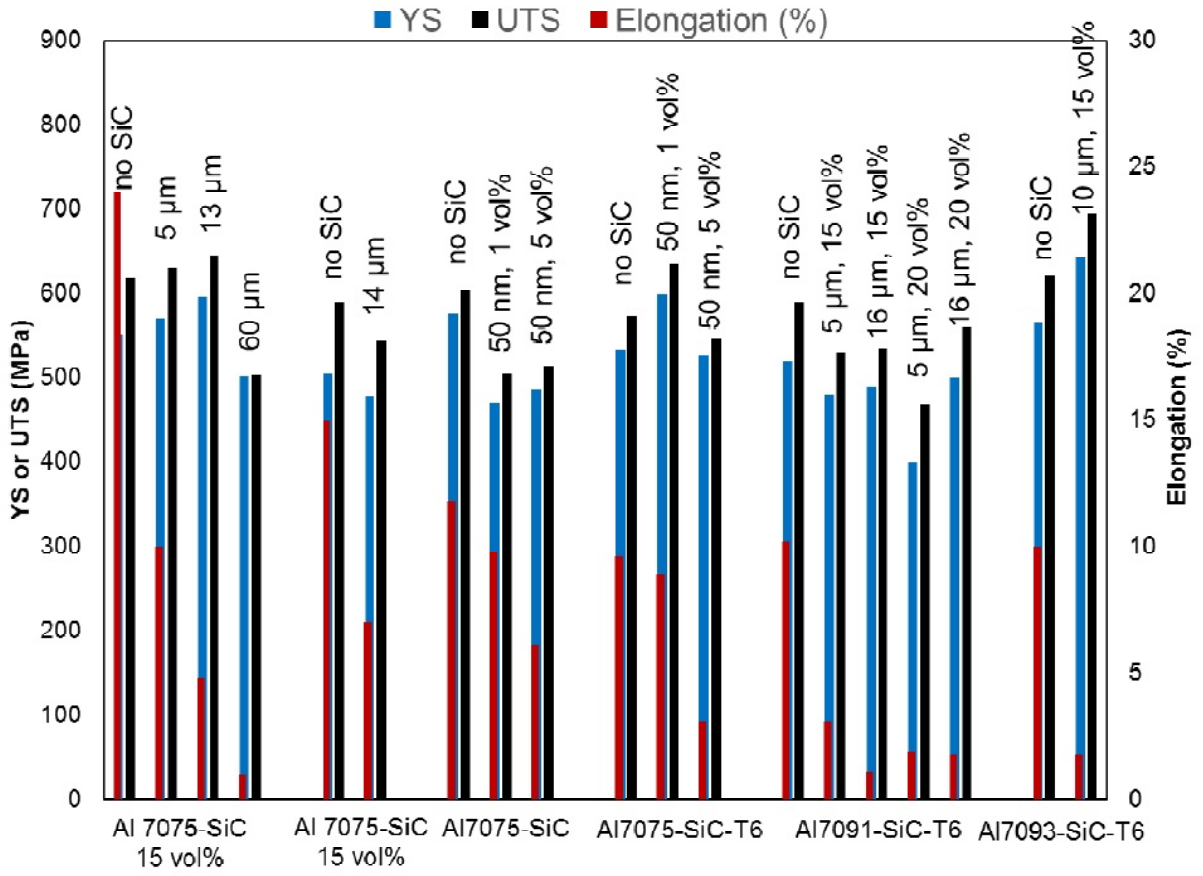

Fig. 7. Tensile properties of select SiC particulate reinforced Al 7xxx series alloy composites. The size and volume percentages of the SiC particles are varied in these studies. Data were obtained from [6,29,31,36,37,60,61].

overaged condition. The difference in fracture toughness and failure mechanisms were not reflected in the tensile ductility. In contrast, 2xxx Al alloy composites only exhibited a marginal effect of matrix aging condition on the toughness, and the 2xxx series composite failed predominantly by particle cracking. However, Doel and Bowen [36] reported that the effects of aging condition on the tensile properties of nano-SiC_p reinforced Al 7075 composites followed the same behavior as those produced in unreinforced material.

Hu et al. investigated B_4C-AA7093 composites synthesized using the Boralyn technique [35]. The microstructural characterization showed MgO particles formed at and near the B_4C/Al interfaces, which resulted in the depletion of the Mg atoms in the matrix and subsequently suppressed the precipitation in the matrix grain interior during the aging process. Likewise, a recent study on a TiO_2-AA7075 composite also revealed the formation of $MgTiO_3$ and ZnO near the matrix/reinforcement interface, which suppressed the formation of Guinier-Preston (GP) zones, resulting in no age hardenability of the composite [64]. Additionally, the thermally-induced dislocations (formed upon quenching from the solution treatment) serve as heterogeneous nucleation sites for precipitate formation in the Al alloy matrix during the aging treatment. A preferential distribution of precipitates in the particle/matrix interface region were observed [17]. The higher density of dislocations also causes an acceleration in the time to peak-aging compared to the unreinforced alloy of a similar composition. An increase in reinforcement volume fraction or a decrease in particle size increases the amount of indirect strengthening from dislocations induced by the reinforcing phase, since a larger amount of interfacial area allows more dislocation punching to take place.

Our recent work on UFG Al 7091 composites reinforced with submicron B_4C particles achieved a promising property combination of YS ~ 650 MPa, UTS ~ 705 MPa and tensile strain at break of ~ 4.1% (Fig. 8), by application of a double-step aging process, defined as T1 temper here, which involves

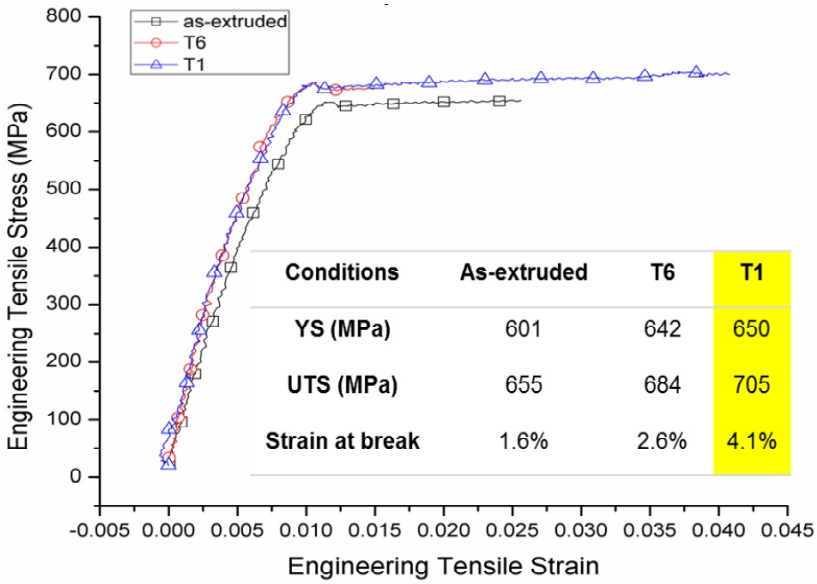

Fig. 8. Tensile stress-strain curves of ultrafine grained Al 7091 composites reinforced with 5 wt.% submicron B_4C particles in different tempering conditions and the corresponding mechanical properties.

artificial aging at 50 °C for 5h followed by a second aging step at 80 °C for 9 h. The microstructural characterization of the composite in T6 temper revealed that rod-like η-$MgZn_2$ precipitates are present in the vicinity of B_4C particles, as illustrated by the dashed oval in Fig. 9. This observation indicated that accelerated aging kinetics occurred in this UFG composite since unreinforced Al 7xxx series alloys typically contain nanoscale GP zones and η' precipitates in T6 temper. It is worth noting that the refining Al matrix grain size also alters the precipitation behavior in this class of Al alloys [64,65]. Additional investigation into the microstructure of this specially tempered composite is ongoing and will be published in another paper. The complexity of microconstituents due to the combination of ultrafine grains, presence of reinforcing particles and thus a high volume of Al/B_4C interfaces needs to be further investigated, in an effort to truly understand the influence of the reinforcement on the microstructural evolution of the heat treatable Al matrix during aging. Presentation of these preliminary data is intended to highlight that the ductility achieved in this UFG Al composites is superior to all of the previous studies on UFG Al composites or nanocomposites, while the strengths are retained at a level above 650 MPa [5,25,34,53]. These preliminary results indicate that careful design of the aging treatment sequence can further improve the mechanical performance of the Al composites using age hardenable Al alloys as the matrix.

4. SUMMARY

A review on the effect of individual microconstituents in Al MMCs on their mechanical performance is provided in this article. Selection criteria of both matrix phase and reinforcement have been discussed. Examination of the existing body of literature shows that evident advances have been achieved in the mechanical properties of the Al MMCs, particularly in the ductility of the composites in recent decades. Earlier studies on ultrafine grained or nanoscale Al composites primarily reported compressive mechanical data and the composites barely exhibited tensile plastic strain. Increasing the volume fraction of coarse grained Al matrix improved the tensile plastic strain while the strength was reduced. Simultaneous enhancement in both strength and ductility has been achieved in recent studies by controlling the spatial distribution of matrix grains and the reinforcing particles at multiple length scales. The size, distribution, and spatial arrangement of the Al matrix grains can be controlled to provide plasticity during deformation. The size and spatial distribution of the reinforcement particles can be tailored to attain various engineering and physical properties. Moreover, the interfaces that form among the various phases also help determine the overall mechanical behavior of the Al composites.

Despite this substantial progress achieved in the field of particulate reinforced Al MMCs, the development of Al composites is still facing challenges in-

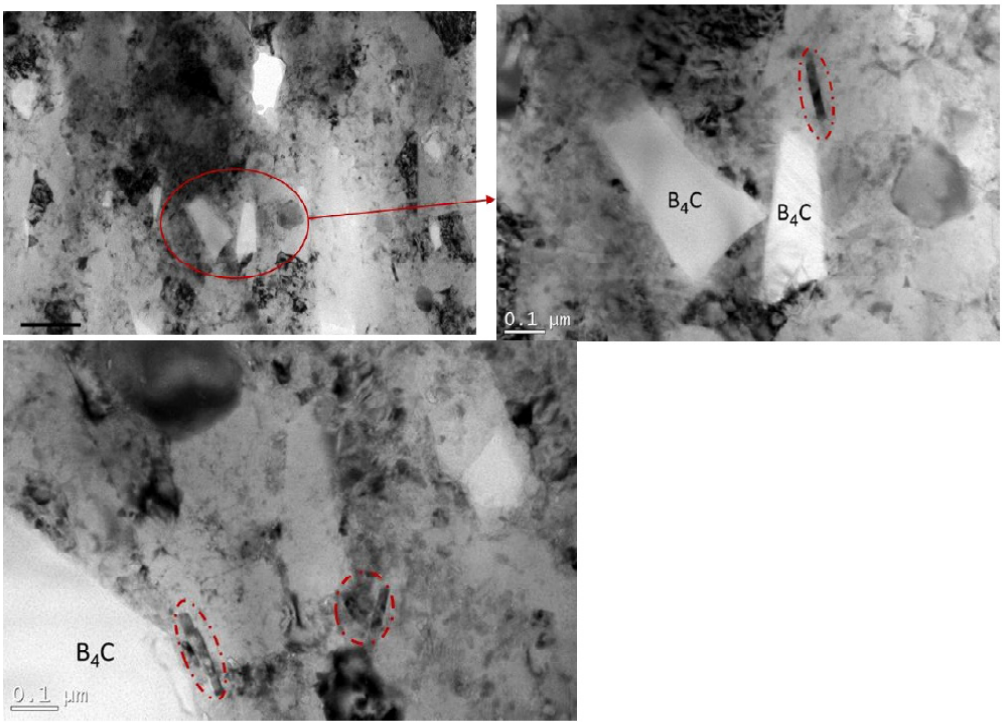

Fig. 9. Representative transmission electron microscopy images of the submicron B_4C particulate reinforced UFG Al 7091 composite in T6 temper. Rod-like η-$MgZn_2$ precipitates are highlighted by the dashed ovals.

clude inferior ductility, low fracture toughness and precise control of the distribution of the different microconstituents during processing. An in-depth understanding of the effect of the reinforcing phase on complex Al matrix alloys such as the families of the age-hardenable Al alloys is in demand, in an effort to optimize the microstructural design of Al composites. In particular, the sensitive dependence of fracture toughness on aging condition reported in the Al 7xxx series composite, in contrast to its relative independence of aging condition in the Al 2xxx series composite, highlights the need to systematically study the effects of matrix microstructure and its role in controlling the microscopic fracture events, which thereby affect the macroscopic mechanical properties. The accelerated aging kinetics due to the presence of the reinforcement particles, especially at or in the vicinity of the Al matrix/reinforcement interface, also suggest that alternative aging conditions, either lower aging temperature or shorter aging times relative to those used for unreinforced counterparts, should be further investigated in an effort to fully achieve the function of the matrix phase in strengthening.

ACKNOWLEDGEMENTS

The authors are grateful for the funding provided by the Office of Naval Research that supported the work by our group reviewed in this article: Grant No. ONR N00014-12-1-0237 under the guidance of Dr. Larry Kabacoff and Grant No. N00014-12-C-0241 under the guidance of Rod Peterson and Bill Golumbfskie.

REFERENCES

[1] M.O. Bodunrin, K.K. Alaneme and L.H. Chown // *J. Mater. Res. Technol.* **4** (2015) 434.
[2] T.S. Srivatsan, T.S. Sudarshan and E.J. Lavernia // *Prog. Mater. Sci.* **39** (1995) 317.
[3] I.A. Ibrahim, F.A. Mohamed and E.J. Lavernia // *J. Mater. Sci.* **26** (1991) 1137.
[4] J.S. Moya, S. Lopez-Esteban and C. Pecharromán // *Prog. Mater. Sci.* **52** (2007) 1017.
[5] C. Suryanarayana and N. Al-Aqeeli // *Prog. Mater. Sci.* **58** (2013) 383.
[6] A. Ahmed, A.J. Neely, K.K. Shankar and S.L.I. Chan // *Mater. Sci. Forum* **561–565** (2007) 761.
[7] Z. Zhang, T. Topping, Y. Li, R. Vogt, Y. Zhou, C. Haines, J. Paras, D. Kapoor, J.M.

Schoenung and E.J. Lavernia // *Scr. Mater.* **65** (2011) 652.
[8] L. Jiang, K. Ma, H. Yang, M. Li, E.J. Lavernia and J.M. Schoenung // *JOM* **66** (2014) 898.
[9] H. Yang, T.D. Topping, K. Wehage, L. Jiang, E.J. Lavernia and J.M. Schoenung // *Mater. Sci. Eng. A* **616** (2014) 35.
[10] T.W. Clyne and P.J. Withers, *An Introduction to Metal Matrix Composites* (Cambridge University Press, 1995).
[11] Z.H. Melgarejo, O.M. Suárez and K. Sridharan // *Scr. Mater.* **55** (2006) 95.
[12] D.J. Lloyd // *Int. Mater. Rev.* **39** (1994) 1.
[13] M. Li, K. Ma, L. Jiang, H. Yang, E.J. Lavernia, L. Zhang and J.M. Schoenung // *Mater. Sci. Eng. A* **656** (2016) 241.
[14] N. Behm, H. Yang, J. Shen, K. Ma, L.J. Kecskes, E.J. Lavernia, J.M. Schoenung and Q. Wei // *Mater. Sci. Eng. A* **650** (2016) 305.
[15] R.J. Arsenault, S. Fishman and M. Taya // *Prog. Mater. Sci.* **38** (1994) 1.
[16] B.S.S. Daniel, V.S.R. Murthy and G.S. Murty // *Process. Adv. Mater.* **68** (1997) 132.
[17] C. Wu, K. Ma, J. Wu, P. Fang, G. Luo, F. Chen, Q. Shen, L. Zhang, J.M. Schoenung and E.J. Lavernia // *Mater. Sci. Eng. A* **675** (2016) 421.
[18] L. Jiang, H. Yang, J.K. Yee, X. Mo, T. Topping, E.J. Lavernia and J.M. Schoenung // *Acta Mater.* **103** (2016) 128.
[19] Q.D. Ouyang, X. Guo and X.Q. Feng // *Mater. Sci. Eng. A* **677** (2016) 76.
[20] J. Ye, B.Q. Han, Z. Lee, B. Ahn, S.R. Nutt and J.M. Schoenung // *Scr. Mater.* **53** (2005) 481.
[21] Y. Li, Y.H. Zhao, V. Ortalan, W. Liu, Z.H. Zhang, R.G. Vogt, N.D. Browning, E.J. Lavernia and J.M. Schoenung // *Mater. Sci. Eng. A* **527** (2009) 305.
[22] Y. Li, Z. Zhang, R. Vogt, J.M. Schoenung and E.J. Lavernia // *Acta Mater.* **59** (2011) 7206.
[23] B. Yao, C. Hofmeister, T. Patterson, Y. Sohn, M. van den Bergh, T. Delahanty and K. Cho // *Compos. Part Appl. Sci. Manuf.* **41** (2010) 933.
[24] V.C. Nardone and K.M. Prewo // *Scr. Metall.* **20** (1986) 43.
[25] A. Ahmed, A.J. Neely, K. Shankar, P. Nolan, S. Moricca and T. Eddowes // *Metall. Mater. Trans. A* **41** (2010) 1582.
[26] M.F. Ashby // *Philos. Mag.* **21** (1970) 399.
[27] S. Scudino, G. Liu, M. Sakaliyska, K.B. Surreddi and J. Eckert // *Acta Mater.* **57** (2009) 4529.
[28] J. Llorca, A. Needleman and S. Suresh // *Acta Metall. Mater.* **39** (1991) 2317.
[29] A.B. Pandey, B.S. Majumdar and D.B. Miracle // *Metall. Mater. Trans. A* **31** (2000) 921.
[30] J.M. Gómez de Salazar and M.I. Barrena // *Scr. Mater.* **44** (2001) 2489.
[31] A. Kalkanlý and S. Yýlmaz // *2nd Int. Conf. Adv. Prod. Process. Alum.* **29** (2008) 775.
[32] V. Balaji, N. Sateesh and M.M. Hussain // *4th Int. Conf. Mater. Process. Characterization* **2** (2015) 3403.
[33] M. Manoharan and J.J. Lewandowski // *Scr. Metall.* **23** (1989) 301.
[34] I. Mobasherpour, A.A. Tofigh and M. Ebrahimi // *Mater. Chem. Phys.* **138** (2013) 535.
[35] H. Hu, E. Lavernia, W. Harrigan, J. Kajuch and S. Nutt // *Mater. Sci. Eng. A* **297** (2001) 94.
[36] T.J.A. Doel and P. Bowen // *Compos. Part Appl. Sci. Manuf.* **27** (1996) 655.
[37] A. Razaghian, D. Yu and T. Chandra // *Australas. Spec. Issue Manuf. Process. Mech. Prop. Characterization Adv. Compos.* **58** (1998) 293.
[38] P. Ashwath and M.A. Xavior // *J. Mater. Res.* **31** (2016) 1201.
[39] M. Ashby, *CES Edupack* (Granta, Cambridge, UK).
[40] R.G. Vogt, Z. Zhang, T.D. Topping, E.J. Lavernia and J.M. Schoenung // *J. Mater. Process. Technol.* **209** (2009) 5046.
[41] R. Vogt, Z. Zhang, E. Huskins, B. Ahn, S. Nutt, K.T. Ramesh, E.J. Lavernia and J.M. Schoenung // *Mater. Sci. Eng. A* **527** (2010) 5990.
[42] D.B. Witkin and E.J. Lavernia // *Prog. Mater. Sci.* **51** (2006) 1.
[43] E.J. Lavernia, B.Q. Han and J.M. Schoenung // *Mech. Behav. Nanostructured Mater. Symp. Held Honor Carl Koch TMS Annu. Meet. 2007 Orlando Fla.* **493** (2008) 207.
[44] H. Yang, E.J. Lavernia and J.M. Schoenung // *Philos. Mag. Lett.* **95** (2015) 177.
[45] K. Wehage, *Tools for Material Design and Selection* (MS Thesis,-University of California, Davis, 2014).
[46] L. Jiang, K. Ma, H. Yang, M. Li, E.J. Lavernia and J.M. Schoenung // *JOM* **66** (2014) 898.
[47] Z. Fan, Y. Wang, Y. Zhang, T. Qin, X.R. Zhou, G.E. Thompson, T. Pennycook and T. Hashimoto // *Acta Mater.* **84** (2015) 292.

[48] W.H. Hunt, C.R. Cook, K.P. Amanie and T.B. Gurganus, In: *Powder Metallurgy Composites*, ed. by P. Kumar, A. Ritter and K. Vedula (The Metallurgical Society, Warrendale, PA, 1987).
[49] R. Z. Valiev, R. K. Islamgaliev, N. F. Kuzmina, Y. Li and T. G. Langdon // *Scr. Mater.* **40** (1998) 117.
[50] A. Borbély, P. Kenesei and H. Biermann // *Acta Mater.* **54** (2006) 2735.
[51] M. Kawasaki, Y. Huang, C. Xu, M. Furukawa, Z. Horita and T.G. Langdon // *Langdon Symp. Flow Form. Cryst. Mater.* **410–411** (2005) 402.
[52] Z. Zhang, T. Topping, Y. Li, R. Vogt, Y. Zhou, C. Haines, J. Paras, D. Kapoor, J.M. Schoenung and E.J. Lavernia // *Scr. Mater.* **65** (2011) 652.
[53] F. Tang, M. Hagiwara and J.M. Schoenung // *Mater. Sci. Eng. A* **407** (2005) 306.
[54] L. Huang, T.D. Topping, H. Yang, E.J. Lavernia and J.M. Schoenung // *Philos. Mag.* **94** (2014) 1754.
[55] S. Tjong and Z. Ma // *Mater. Sci. Eng. R Rep.* **29** (2000) 49.
[56] T. Ram Prabhu // *Arch. Civ. Mech. Eng*. **17** (2017) 20.
[57] H.X. Peng, Z. Fan and J.R.G. Evans // *Mater. Sci. Eng. A* **303** (2001) 37.
[58] R. Rodrýěguez-Castro, R.C. Wetherhold and M.H. Kelestemur // *Mater. Sci. Eng. A* **323** (2002) 445.
[59] C.-Y. Lin, H.B. McShane and R.D. Rawlings // *Mater. Sci. Technol.* **10** (1994) 659.
[60] Jian Ku Shang and R. Ritchie // *Acta Metall*. **37** (1989) 2267.
[61] L.E.G. Cambronero, E. Sánchez, J.M. Ruiz-Roman and J.M. Ruiz-Prieto // *Proc. Int. Conf. Adv. Mater. Process. Technol*. **143–144** (2003) 378.
[62] D. L. McDanels // *Metall. Trans. A* **16** (1985) 1105.
[63] S.R. Nutt and R.W. Carpenter // *Mater. Sci. Eng*. **75** (1985) 169.
[64] R. Karunanithi, K.S. Ghosh and S. Bera // *Metall. Mater. Trans. A* **45** (2014) 4062.